EECE-Faculty of Engineering
Cairo Universtiy

IonoCrafts

Research Paper

by

We Scare Because We Care

team

9220426	عبدالرحمن بدوي محمد طاهر
9220785	محمود عبدالسلام عبدالصادق عبدالفتاح صقر
9220535	عمر خالد عبد العال محمد
9220473	عبدالرحمن محمد صلاح الدين ابوهندى
9220419	عاصم حسين محمد محمد
9220774	محمود تامر علي
9220849	مصطفى محمد مصطفى السلكاوى

Supervisor

Dr Samah El-Shafiey

1 Abstract

This study intends to investigate the viability of developing an ionocraft—an aircraft that is propelled by electric thrust—by utilizing the corona discharge phenomenon and the Biefeld-Brown effect. We carried out a thorough analysis of the Biefeld effect, how earlier research took advantage of the corona to aid in their work, and how we may support this endeavor.

Our model's primary goal is to thoroughly examine all of the factors influencing the simulation and hardware outcomes by analyzing the geometry, presumptions, governing equations, and boundary conditions. The development of the ionocraft's structure and the design of a high-voltage power supply are two examples of the hardware implementation covered by the technique. We have included simulations with MATLAB, CST, and Comsol in our package. The findings from hardware experiments and simulations utilizing the aforementioned software are the main focus of the analysis and results.

Ultimately, the report ends with recommendations for additional research The purpose of this research article is to further our understanding of ionocraft technology, which has potential uses in a range of aerospace and propulsion applications.

Contents

List of Figures

List of Tables

2 Introduction

Pollution caused by the aircraft industry is a lot and this industry has a lot of problems like aircraft noise which is considered one of the main sources of noise pollution[1] which directly has a lot of consequences and damages health, this made them set standards to the limit of noise caused by aircraft and drones, air pollution is also a very serious problem caused by the aircraft and other vehicles, according to IATA air transport is responsible for 2% of global energy-related CO_2 emission [2], this is a lot considering the number of flights, in addition, maintenance of any mechanical part that has moving parts, complex design and functionality is a major problem in aircraft so they may try to make less moving parts or make them one part.[1]

The proposed solution to these problems is ion-propelled aircraft these aircraft have the following properties: low noise, no CO_2 emissions, no moving parts, and it is used in applications such as micro-drones, less-than-air aircraft, cooling systems, and most importantly drones.[1] the idea of moving or flying using ion propulsion started in space crafts and satellites, NASA sees that ion propulsion is the key to deep space.[3]

Imagine a spaceship that zips around space like a silent ballerina, not with fire and explosions of fuel, but with ions. These ions get pushed out the back of the spaceship with acceleration using voltage difference, making it go forward.

It's the same trick with airplanes, but instead of storing the ions we will use air that's already there, ionize it then accelerate it using an electric field pushing the aircraft up into the sky. So, whether it's flying through the stars or bouncing through the clouds.

A very common and basic system of ion propulsion is ionocraft or lifer, generally, it consists of two electrodes one is sharp (wire in lifter example) and the other is round (aluminum foil in the lifter example) when applying an external high voltage between the two electrode the air around the positive electrode will be ionized and then accelerated because of the electric field making ion wind, this wind produces a thrust that makes the lifter fly this is called Biefeld–Brown effect.[4].

Before diving into the paper we want to identify some terms that will be mentioned a lot.

- Thruster: System that gains thrust by throwing mass in the other direction
- EAD thruster: Thruster that uses the air ions to gain reaction force.

3 Literature Review

We investigated recent papers about the EAD thrusters and the Biefeld-Brown effect, we found the history of the EAD thrusters, theories, models, and various types of EAD thrusters.

3.1 Historical review

Electroaerodynamics (EAD), also known as electrohydrodynamics (EHD), has been adapted and developed as a clean engine to address the issue of pollution produced by the engines of regular airplanes, rockets, and spacecraft. Christenson and Moller conducted the first experimental study on EAD propulsion for in-atmosphere application in 1967. They could demonstrate how EAD could produce thrust through theoretical and experimental analysis[5].

This was not the exact moment the idea was born; rather, it was in Ohio in 1920 that young Thomas Townsend Brown, an American physicist, saw a tiny vibration in a Coolidge X-ray tube while conducting a series of experiments with the tube. A few quantitative experiments later, he was able to validate his theory. After his idea was rejected for some time, physicist Alfred Biefeld from Switzerland became his supervisor, and their theory—dubbed the ”Biefeld-Brown effect”—became known[5].

For the next sixty years, T.T. Brown carried out experiments on his effect, recording his design efforts mainly through the filing of patents, the most notable of which are patents 2,949,550 and 3,187,206. (1960, 1965, Brown) Figure 1 illustrate two significant categories of experimental activity that are represented by these patents[6].

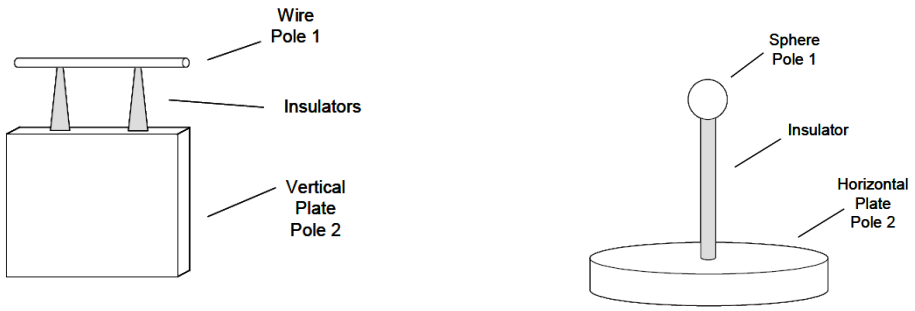

(a) Patent 2,949,550. **(b)** Patent 3,187,206.

Figure 1: T.T. Brown’s Primary Electrokinetic Patents (Brown, 1960, 1965)[6]

However, this effect remained improperly appreciated until the 1990s when NASA unfolded it. It has become a hot topic again as at the same time some scientists were working on some rigorous proofs concerning this effect.

In recent years, a large number of publications were published in this field, more theories were

presented, and more sources attribute the effect to corona ionic air propulsion, but so far, no satisfactory explanation has been presented to fully describe the effect.

Ion propulsion represents an innovative and groundbreaking propulsion method that harnesses electrohydrodynamics (EHD) for generating thrust. EHD involves the examination of the interplay between electric fields and fluids [7].

3.2 Biefeld-Brown effect mechanism and proposed theories

The fundamental steps outlining the ion propulsion process are as follows:

An elevated direct current (DC) voltage is administered to the electrodes of an asymmetric capacitor, this results in the creation of a potent electric field between these electrodes, the formidable electric field leads to the ionization of the surrounding air or fluid, generating a cloud of positively charged ions and negatively charged electrons, the ion cloud gets propelled by the electric field existing between the electrodes, with positive ions being accelerated toward the negative electrode, this acceleration of ions gives rise to a flow of charged particles, termed an ”ion wind”, the ion wind interacts with the neutral air molecules around it, transmitting a portion of its momentum to these molecules, this momentum transfer yields a thrust force acting on the ionocraft [1].

The main phenomenon that contributes to ion propulsion is corona discharge is characterized as an electrical discharge occurring when a high voltage is applied to a sharp or pointed electrode. Corona discharge can ionize the air surrounding the electrode and potentially generate ozone gas, necessitating the use of a thin electrode [1].

To understand the Biefeld-Brown phenomenon There are two proposed theories:

Ion wind theory

According to the ion wind theory, the lift on an ionocraft is generated by the ionization of air by a strong electric field. However, experiments by Bahder and Fazi have shown that this theory can only explain a small fraction of the observed lift. The lift predicted by the theory is at least three orders of magnitude greater than what is observed[8]. This suggests that the ion wind theory cannot be the primary source of lift on an ionocraft.

Ion drift theory

Researchers posit that ions will have a significant yet indirect influence on this phenomenon, which is also the underlying reason for the inadequacy of the ion wind explanation. The ion drift theory factors in various indirect factors, including ion collisions. According to calculations conducted by Thomas B. Bahder and his research team, this theory yields results that are notably more precise than the ion wind theory, as outlined in their study [8].

3.3 Types of EAD Thrusters

Exposed coupled thruster

A very common and basic thruster consists of two electrodes one is sharp and the other is round and fluid between them, it can take many shapes round triangular, or square.

This Architecture has proven that the ion wind is a function of its structure parameters like the voltage applied, the radius of the electrodes, and the gap between them but, the height of the cathode is not significant in the values of thrust[9]. Another important observation was made in the simulations that the maximum ion wind produced is at the ends of the electrodes instead of the gap area [9]. Ma Chen et al [10] proposed a surface-aerodynamics-based model for exposed decoupled, they proved the completeness of their model but they didn't solve it, but they did experimental work, the structure used for the model was an ionocraft lifter, they found that the thrust produced was very low around 5g lift, they also found that there is a linear relation between the thrust and the length of the electrode which shows the existence of good symmetry in this direction.

Exposed decoupled thruster

In this thruster ion generation and ion acceleration are decoupled (ion generation is done by an AC source), the anode set of electrodes consists of two electrodes one is encapsulated by a dielectric material, and the other is exposed to the distance between these electrodes is small (in order of micrometers)[11].

The studies conducted by Xu et al [12, 13] focused on comparing Dielectric Barrier Discharge (DBD) and corona discharge ion propulsion. They found that DBD-based propulsion systems can achieve approximately twice the Thrust Power ratio of Corona discharge ion propulsion. Additionally, in 2021 [13], the same research team presented an empirical model for thrust and power dissipation. They discovered that the drift current responsible for thrust, when using fixed DC parameters such as DC voltage and electrode gap, depends solely on the AC power, not on voltage nor frequency. This finding implies that the thrust magnitude can be controlled independently of the DC parameters, and reasonable thrust levels can be attained even with lower DC voltages.

In another study by Brown et al [11], researchers designed and tested an exposed decoupled ion-propelled aircraft for practical surveillance missions. They utilized arrays of electrode pairs to generate thrust. The results from their design indicated that exposed coupled or decoupled thrusters have limitations in providing practical climb for surveillance aircraft. They demonstrated that their design, using exposed Electrohydrodynamic (EAD) propulsion, can achieve stable ascent during calm days or calm dawn conditions. Based on these findings, they continued to explore another design using ducted thrusters.

Ducted thrusters

Ducted Electrohydrodynamic (EHD) thrusters can consist of one or more EHD electrode pairs. When multiple stages of electrodes are used in such thrusters, they are referred to as multi-staged ducted (MSD) thrusters. According to the study by Brown et al [11], MSD thrusters are both more powerful and more efficient compared to their exposed counterparts.

Some hypothesized advantages of MSD thrusters as discussed in the same study include:

- The duct can provide support for the electrodes, allowing them to be made smaller, which in turn reduces drag losses.
- The duct can act as a physical barrier between the electrodes and the surrounding environment. This barrier may enhance safety, as it reduces the likelihood of accidental electrical shocks to humans from the electrodes [11].

For a fixed thruster gap spacing and voltage, a ducted thruster produces approximately 3.5 times as much thrust as an equivalent unducted thruster; the thrust-to-power is doubled. This is the main advantage of ducting for EHD thrusters: the duct contributes to thrust, increasing both thrust and efficiency.

To summarize, Ion propulsion is a new and exciting technology with the potential to revolutionize the way we travel. It is silent, has no moving parts, and is very efficient. However, ionocraft is still in the early stages of development, and several challenges need to be overcome before they can be commercialized.

One of the main challenges is that ionocraft requires a high-voltage power source. Another challenge is that ionocraft is very delicate. The electrodes are very thin and can be easily damaged. Despite these challenges, ionocraft has the potential to be a new and revolutionary form of propulsion for aircraft. If the challenges can be overcome, ionocraft could revolutionize the way we travel.

In addition to their potential for terrestrial transportation, ionocrafts are well-suited for planetary exploration. Ion thrusters produce more thrust in lower-pressure environments and can operate in different atmospheric compositions, regardless of the polarity of the produced ions [7]. This means that ionocraft could be used to explore planets with thin atmospheres, such as Mars, without the need for propellants that are sensitive to the atmosphere's composition.

4 Mathematical Modelling

We aim to understand a particular phenomenon by presenting three mathematical models and conducting tests to determine the parameters of an ionic lifter. Additionally, we explore methods for optimizing the lifter's output and measuring its efficiency.

4.1 Model: Wire to cylinder lifter

In this model, the focus is on a wire formed circularly above the cathode. The processes of ion formation and force calculations are analyzed independently to gain a comprehensive understanding of their dynamics.

We focus on the charge density of the area in our equations, and this time we take into consideration the ionized region and use these equations to get the voltage.

4.1.1 Geometry of the model

Our setup for the model consists of three main components:

- Wire electrode.
- Aluminum foil electrode.
- The space between 2 electrodes (air).

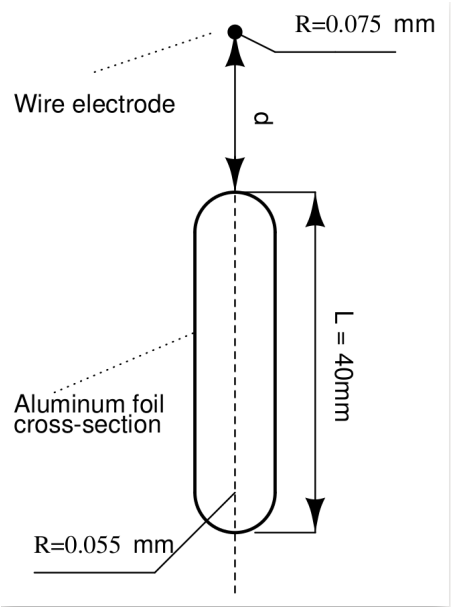

Figure 2: A cross-section of Model 2

4.1.2 Assumptions

There are some assumptions we take into consideration to model our problem:

- the reduced electric field is relatively low.
- conduction is superior to convection and ion diffusion.
- The fluid is incompressible laminar in the drift region.
- The incompressible flow decouples the energy conservation from the momentum equation.
- Fixed air.

4.1.3 Governing Equations

In our model we consider electrostatic interaction between electrodes and the space charges, the moment exchange, induced flow, the structural pressure, and viscous resistance. Three main equations govern our problem:

1. Poisson equation which determines the potential distribution:

$$\nabla^2 V = -\frac{\rho_q}{\varepsilon_0} \tag{4.1}$$

   where:

   * V is the potential distribution.
   * ρ_q is the space charge distribution.
   * ε_0 is the permittivity of free space.

2. Current Density Equation:

$$\mathbf{J_i} = \mu_i \mathbf{E}\rho_\mathbf{q} + \rho_q \mathbf{E} - D_i \nabla \rho_q \tag{4.2}$$

   where:

   * $\mathbf{J_i}$ is the current density.
   * $\mathbf{E}_{\rho_\mathbf{q}}$ is the electric field.
   * mu_i is the mobility of ions.
   * D_i is the diffusion coefficient of ions.

3. Navier-Stokes Equation (conservation of mass and conservation of momentum):

$$\rho(\mathbf{u}\cdot\nabla)\mathbf{u} = -\nabla p + \nabla\left(\nabla\mathbf{u} + (\mathbf{u})^T\right) + \mathbf{F} \tag{4.3}$$

Where:

* $\mathbf{u}$ is the velocity of air.
* ρ is the density of air.
* F is the viscosity of air.
* p is the pressure.

From the assumption that conduction is superior to convection and diffusion, equation 4.2 becomes:

$$\mathbf{J_i} = \mu_i \mathbf{E}\rho_\mathbf{q} \tag{4.4}$$

From the assumption that the fluid is incompressible and laminar, equation 4.3 becomes:

$$\rho_q \mathbf{E} = \nabla p \tag{4.5}$$

From the assumption of a steady-state current meaning that:

$$\nabla\cdot\mathbf{J_i} = 0 \tag{4.6}$$

Putting eq.4.4 in eq.4.6 yields:

$$\nabla\rho_q\cdot\nabla V = \frac{\rho_q^2}{\varepsilon_0} \tag{4.7}$$

Now the main equations to be solved are eq.4.1 and 4.7 to get the potential and charge distribution, The electric field can be easily obtained from:

$$\mathbf{E} = -\nabla V \tag{4.8}$$

Using the resultant electric field to get the gradient of the pressure (the force) using eq4.5.[14].

4.1.4 Boundary Conditions

1. Electric field strength on the surface of an ideal smooth cylindrical.

$$E_p = E_o\delta\varepsilon(1+0.308\sqrt{\delta r_c}) \tag{4.9}$$

Where:

* E_p is the electric field strength (V/m).
* E_o is the air breakdown electric strength $(3.31 \times 10^6 V/m)$ [14].
* δ is the relative air density $(298p/T)$.
* r_c is the wire electrode radius (m).
* T is the temperature $(293.15K)$.

2. Surface charge density:

$$\sigma = \varepsilon_0 E_p \tag{4.10}$$

Where:

* σ is the surface charge density (C/m^2).

3. Electric field in the ionization region:

$$E(r) = \frac{E_p r_c}{r} \tag{4.11}$$

Where:

* E(r) is the electric field at radial position r (V/m).
* r_c is the wire electrode radius (m).

4. Ionization region radius:

$$r_i = r_c \delta (1 + 0.308 \sqrt{\delta r_c}) \tag{4.12}$$

Where:

* r_i is the ionization region radius (m).

5. Voltage applied to the wire electrode surface:

$$V_i = V_c - E_p r_c \ln(\frac{E_p}{E_o}) \tag{4.13}$$

Where:

* V_i is the voltage applied to the wire electrode surface (V).
* V_c is the voltage planned to be applied to the wire electrode (V).

5 Methodology

The methodology is divided into two parts: Software simulation and Hardware implementation of the ionocraft to test the simulation:

5.1 Software Simulation

We attempt to Solve the governing equations using three different software:

1. Using Matlab.
2. Using COMSOL Multiphysics.
3. Uising CST.

5.1.1 Matlab Simulation

we attempt to solve the governing equations using Matlab, using finite different methods.

To solve using the finite difference method we must specify grid and mesh, finite difference approximation of main equations and Boundary conditions.

We chose a grid of $60 \times 2mm^2$, the number of divisions in the x-direction is 150 divisions, and in the y-direction is 1000, there is no z-direction because of symmetry conditions.

The mesh used is non-uniform, where the mesh size is smaller in regions near electrodes and wider in free regions fig.3, this makes the simulation accurate and fast at the same time. Equations and boundary

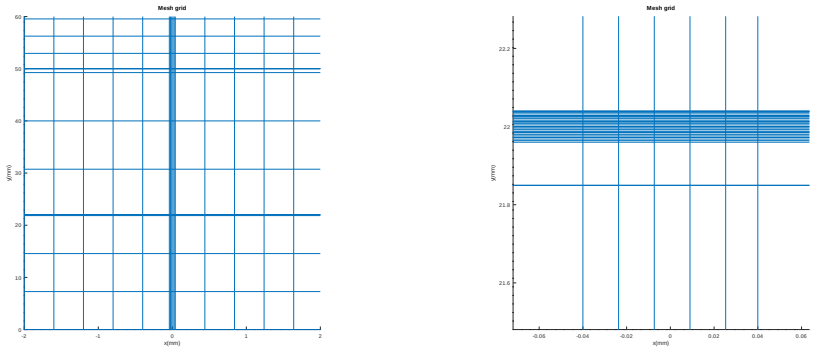

(a) Full grid (b) Zoomed around electrode

Figure 3: non-uniform mesh, more dense around electrodes.

conditions must be written in finite difference approximation form.

1. Poisson Equation eq.4.1:

$$V_{i,j} = \frac{1}{2} * \frac{1}{(\frac{1}{dx})^2 + (\frac{1}{dy})^2} * \left(\frac{V_{i+1,j} + V_{i-1,j}}{dx^2} + \frac{V_{i,j+1} + V_{i,j-1}}{dy^2} + \frac{\rho_{q_{i,j}}}{\varepsilon_0} \right) \tag{5.1}$$

Where:

* dx is the mesh size in the x-direction.
* dy is the mesh size in the y-direction.

Here dx and dy is not the same and is not constant over the full grid.

2. approximation of equation 4.7

Since we assumed low ionization, we can ignore the effect of charges and ignore equation 4.7 and equation 5.1 will be

$$V_{i,j} = \frac{1}{2} \times \frac{1}{(\frac{1}{dx})^2 + (\frac{1}{dy})^2} \times \left(\frac{V_{i+1,j} + V_{i-1,j}}{dx^2} + \frac{V_{i,j+1} + V_{i,j-1}}{dy^2} \right) \tag{5.2}$$

Lastly, to calculate dx and dy:

$$dx = X_{i+1,j} - X_{i,j} \tag{5.3}$$

$$dy = Y_{i+1,j} - Y_{i,j} \tag{5.4}$$

Now we will define the boundary conditions of the model.

1. Wire Electrode:

$$x^2 + (y - y_1)^2 < rc^2 \tag{5.5}$$

Where:

* rc is the wire electrode radius.
* y_1 is the position in the y-direction and is chosen to be 50.

2. Aluminum foil (Collector Electrode) :

$$y < \sqrt{ft^2 - x^2} + y_2 \tag{5.6}$$

Where:

* ft is the foil radius or thickness.

* y_2 is the position in the y-direction and is chosen to be 50 - gap distance.

3. Voltage at boundaries:
   at boundary described by eq .5.5 , Voltage is given by Kapztov peek Law eq. 4.9 and eq. 4.13.
   And at the boundary described by eq. 5.6 Voltage is 0 also at the boundaries of the grid Voltage is 0.

Now all the boundaries and equations are specified, Nothing is left but to solve them.

5.1.2 Simulating the model using Comsol

Simulating the model using the Corona discharge previously defined package in Comsol was somehow a challenging task, but we could get some results as we did the following:

1. Studying the plasma module (the module specified to simulate corona discharge).
2. Defining the constants and parameters usually used in the simulation.
3. Setting all the required chemical reactions, including:
   (a) Electron impact reactions.
   (b) Surface reactions.
4. Setting the initial values.
5. Setting the boundary conditions.
6. Adjusting the meshing to solve by finite volume method (which is preferable for the software).
7. Adjusting time dependency to take results in different instants.

5.2 Hardware Implementation

There are two types of simple lifters: coupled and decoupled. The collector electrode and corona wire of a coupled ionocraft are connected directly to the high-voltage power supply. Although it is simpler to use, this kind of ionocraft might be less effective[15]. A decoupled ionocraft, on the other hand, controls the voltage provided to the corona wire using a different control circuit. Although they are more difficult to operate, decoupled ionocrafts can provide increased stability and efficiency. We shall concentrate on the coupled ionocraft for our implementation.

In fig.4, a block diagram of the coupled ionocraft structure:

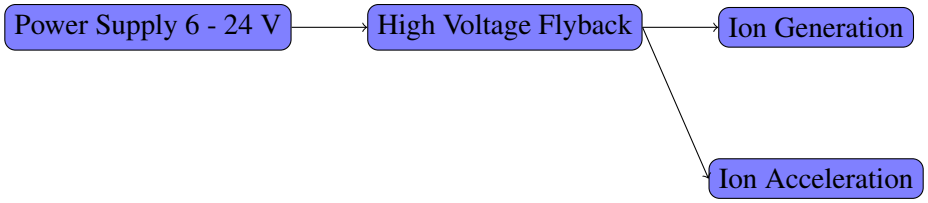

Figure 4: Block diagram of the hardware process

Three primary parts make up an ion propulsion system: an air gap, an emitter wire (corona), and a downstream-positioned collector wire or strip. For maximum thrust and achieving a saturated corona current condition, the emitter and collector should be positioned as close to each other as feasible to create a narrow air gap but ensure there will be no arcing[16]. The ionocraft structure and a high-voltage power supply are the two main parts of an ionocraft. The implementation phases depend on whether the ionocraft structure is exposed-coupled (corona) or exposed-decoupled (DBD).

The electrical energy required to produce ionized air and drive the ionocraft is supplied by the high-voltage power source. Although alternating current (AC) and direct current (DC) power sources can be utilized, DC power supplies are typically chosen because of their efficiency and simplicity.

Typical components of a DC high-voltage power supply include the following:

- Low voltage power supply: Offers 6 to 24 volts as an input voltage.
- Transistor: Controls the flow of current.
- Voltage divider: Splits the voltage to get the appropriate amount.
- Flyback Transformer: Increases input voltage to the necessary high voltage level step by step.Older cathode-ray tube (CRT) televisions frequently include flyback transformers.

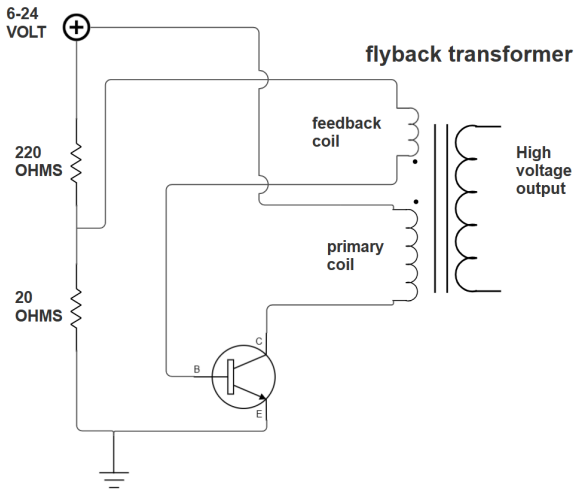

Figure 5: Implementation circuit of high voltage generator

The actual configuration of the electrodes that produce ionized air is referred to as the ionocraft structure. The ”lifter” which usually comprises a triangular or circular frame with a suspended corona wire (thin wire electrode) above it, is the most basic sort of ionocraft structure. The collector electrode is the frame.

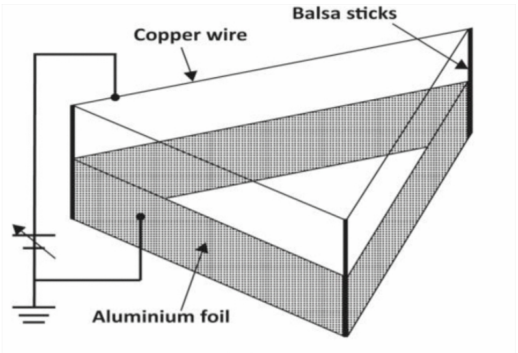

Figure 6: The lifter design

These Quantities are to be measured in our experiments:

1. Power dissipation: it could be measured

$$P = V_{in} \times I_{in} \tag{5.7}$$

   Where:

   * V_{in} is the input voltage and I_{in} is the input current.

2. Thrust/Lift: Due to a lack of fine equipment the following method is used, we load the ionocraft with some weight and when the ionocraft reaches equilibrium the weight of the ionocraft is measured using a sensitive scale.

3. Gap distance: since the gap distance measured in centimeters, it is safe to measure it using a regular ruler.

Additional Considerations

Based on the particular needs of the application, the power supply and ionocraft structure should be selected. The reduction of electrical discharge risk should be the top priority when designing the ionocraft's structure. Adhering to appropriate safety protocols is imperative while handling high-voltage electrical equipment.

6 Hardware Results

In the modeling section, we referred to two models to be studied: one was ideal and was only to understand the pure core of the Corona discharge phenomenon and how to exploit it well, and the other was the realistic one, from which all our results and analysis will diverge.

The model of wire to cylinder lifter

In our analysis of this model, we considered four different methods and aimed to compare the results between them to get a good sense of the so-far accurate details of how the lifter works.
The scenarios we adopted to get the results were based on four pillars, as follows:

1. **Hardware implementation of the lifter**

   The objective was to implement the lifter physically and obtain accurate results by measuring the thrust generated.

2. **Simulating the model using Comsol**

   This method involved utilizing numerical methods to solve the equations adopted by the model, enabling the accurate determination of thrust and the plotting of results.

3. **Simulating the model using CST**

   This method relied on predefined software packages designed for simulating corona discharge. The focus was on simulating the model using these tools and parameters.

4. **Solving the equations using Matlab**

   This method closely resembles the previous one, as it aimed to employ multiple simulation tools, including Comsol, to address the challenges encountered during the simulation process.

6.1 Hardware Experiment

To perform the Experiment, the First thing is the high-voltage generator, then the structure itself, and lastly measurements.

6.1.1 High voltage generation

we have implemented the high voltage power supply circuit that was discussed in the methodology with an input voltage of 12 volt.

6.1.2 Experiment Tests:

1. Test 1:

   In test 1, we prepared a Triangular ionocraft with a side length of 10 cm, and aluminum foil height of 4cm,with wooden skewers as support. The voltage applied $\approx 30KV$ (we couldn't measure it accurately due to the loading effect, but the arc established at around 1cm). Unfortunately, the ionocraft didn't fly, the ionocraft was too heavy to take off, and the thrust was too weak. First, we try to increase the input voltage from 12 volts up to 19 volts, but unfortunately, the thrust was too weak to make the ionocraft fly, we couldn't measure the thrust of due to a lack of equipment and the ionocraft is still fixed.

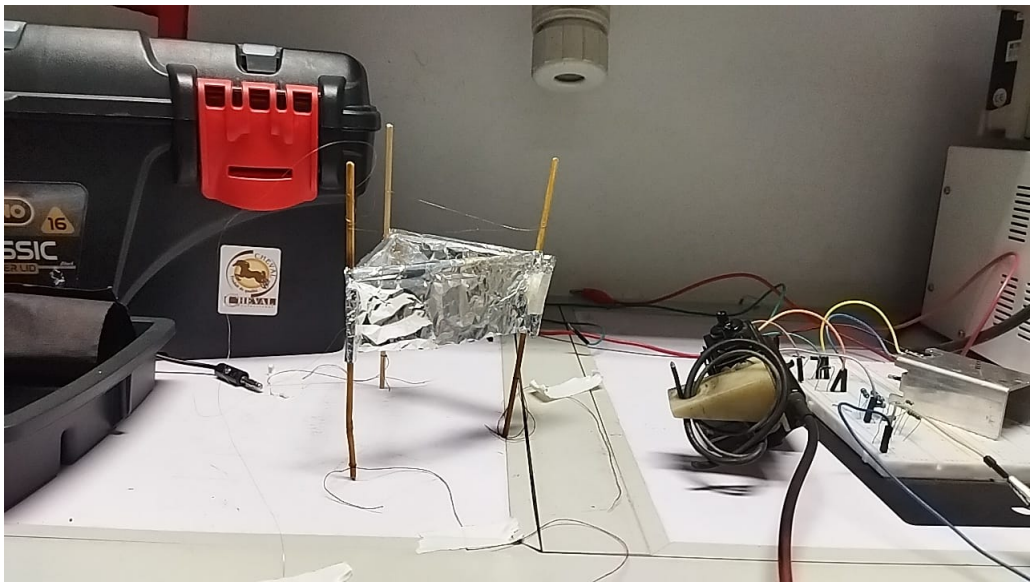

Figure 7: Setup 1 Triangular ionocraft with wooden skewers support

Input voltage	12:19V
Length	10cm
Foil height	4cm
Wheigh	7.6gm

Table 1: Specifications of test 1.

2. Test 2:

   In this test we made the following changes: the wooden skewers were replaced by plastic straws, the length of the support was reduced, and the height of the aluminum foil was reduced, and the input voltage was increased to 30 volts.

   Unfortunately, the ionocraft didn't fly, although the thrust was stronger

   Now, we may make changes to the circuit generating the High voltage itself, We should also change the measuring technique of thrust, to allow for measuring weak Lifts even when the ionocraft is on the ground.

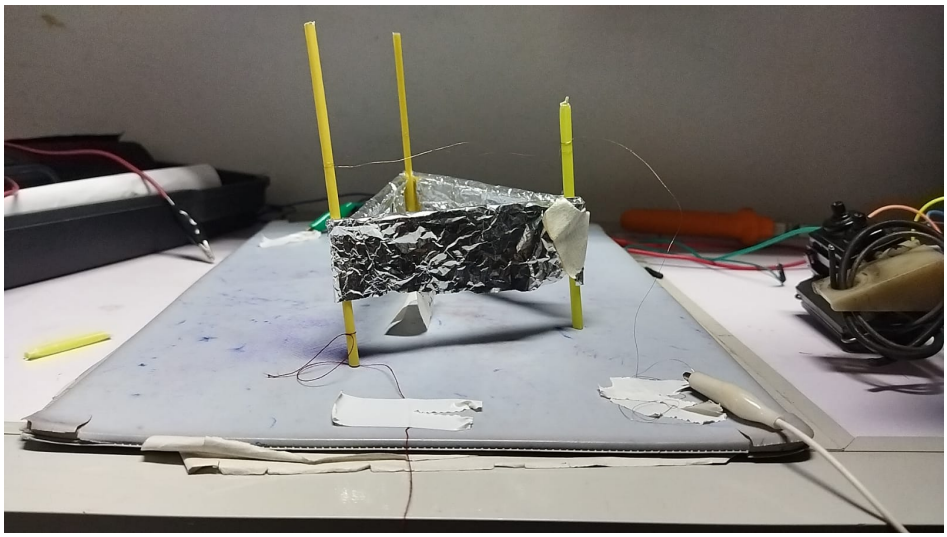

Figure 8: Setup 2 Triangular ionocraft with plastic straws

Input voltage	30V
Length	10cm
Foil height	2cm
Wheigh	2.7gm

Table 2: Specifications of test 2.

7 Simulation Results

Now, we will test the previous three simulation methods in three different simulation programs.

7.1 Result of simulation with matlab

We simulate only testing scenarios one for Applied Voltage and the other for Gap distance, with the output average Velocity.

1. Voltage Vs Velocity:

   We Varied the Applied Voltage from 18KV to 23KV and calculated the average velocity of air in the region $28mm \times 0.26mm$, with gap distance $d = 28mm$ and electrode radius $rc = 0.075mm$ and foil (Collector) thickness $0.01mm$. the results are shown in fig9.

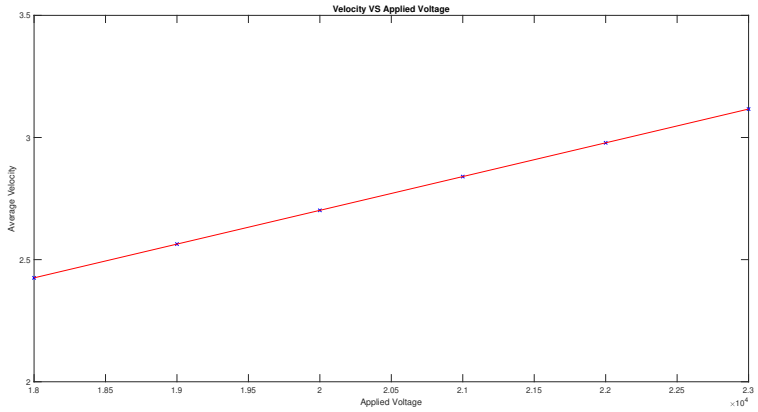

Figure 9: Voltage Vs Velocity, linear relationship

the output velocity shows an incremental linear relationship with the applied velocity, this is a good sign for the simplicity of our model. the slope of the line is $0.13822(m/s)/(KV)$ Comparing the results with experimental data [14], Fig.10. as shown in Fig.11, the Simulation fits with Experimental data quite well with a Relative error of = 0.7144%

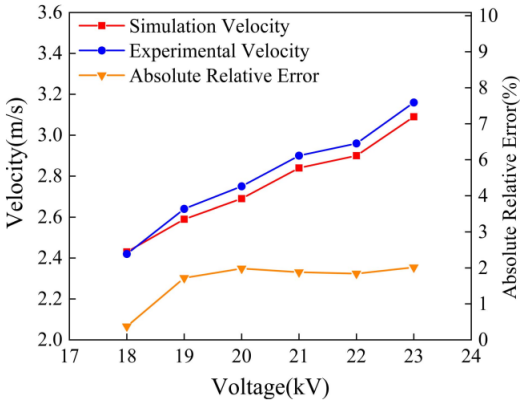

Figure 10: Experimental data [14]

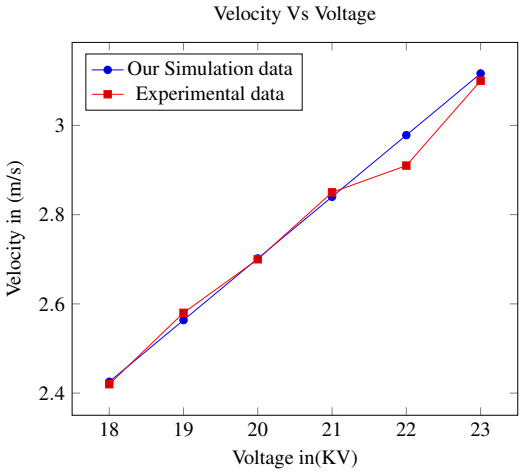

Figure 11: Velocity Vs Voltage, Comparison with experimental data

2. Velocity Vs gap distance The second case, we varied the gap distance from 26mm to 30mm, with constant applied Voltage of 20KV and $rc = 0.075mm$, the results are shown in Fig.12 the results show an incremental inverse relationship between Velocity and gap distance, again this simple relationship is a consequence of our simplified model.

   Comparing the data with Experimental data[14] in fig.13 the results of the Comparison are shown in Fig.14, the figure shows agreements for gap distance less than 32, which means that our model doesn't behave well for larger gap distances the relative error is 1.66% for values less than 32 gap distances and the total relative error is 6.012% which is still not so bad.

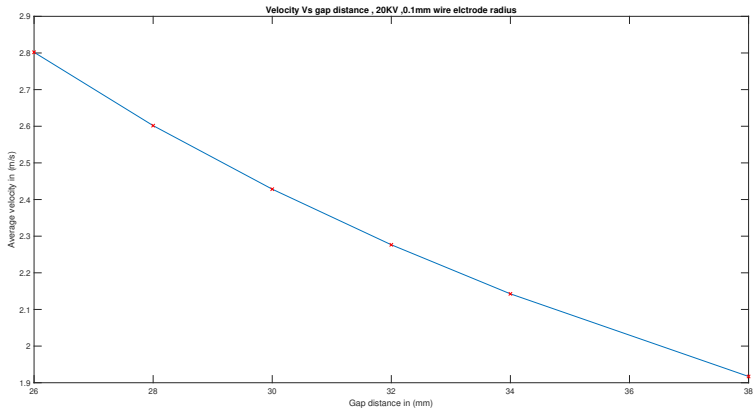

Figure 12: Velocity Vs gap distance, Simulation data

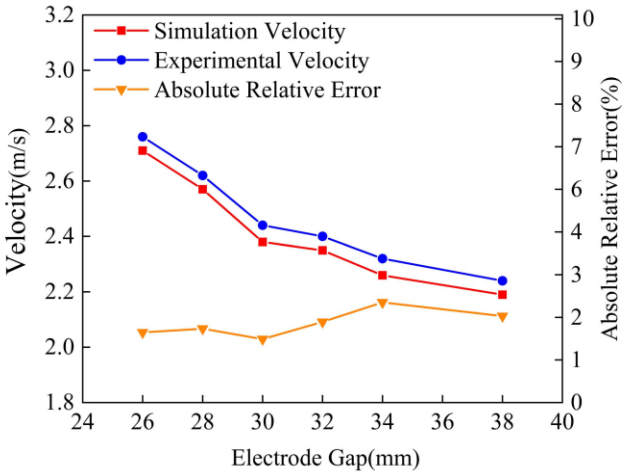

Figure 13: Velocity Vs Gap distance,Experimental data [14]

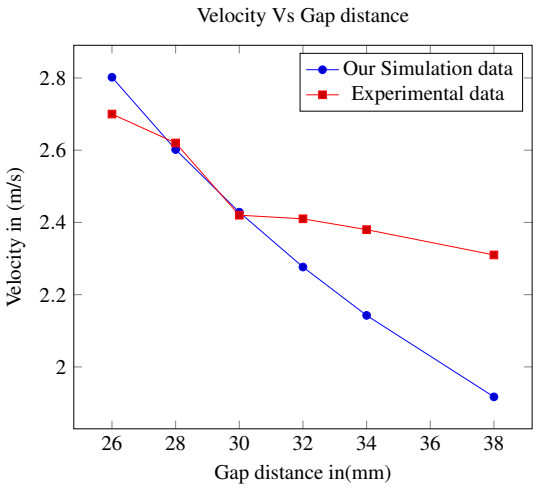

Figure 14: Velocity Vs Gap distance, Comparison with real data

7.2 Results of simulation with Comsol

Truning to Comsol, we could get results, but what was disappointing is that we couldn't get results except for the 1D model, as the other 2D and 3D models have failed due to both technical and informatics problems.

From these results, we could calculate the current density at the applied voltage we did in the hardware and got to compare them in the analysis section.

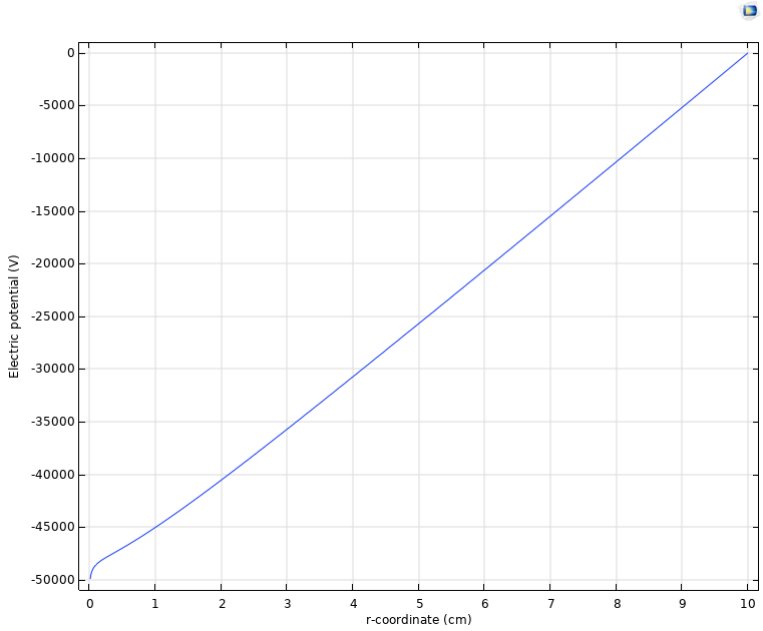

Figure 15: Electric potential vs r coordinate support

7.3 Results of simulation using CST

This method is being mentioned just to record the numerous tries we made to use this software (CST), but all of it came to a bad end.

1. We started to draw the unit of the lifter wire and the aluminum foil.
2. We can't set the voltage to a non-PEC martial.
3. We set both the wire and aluminum foil into PEC and imagine it as an approximation.
4. We take the steps into initializing the system and boundary conditions.
5. Due to limited knowledge and time when simulating no results output because of an error that connects the two PECs.

7.4 Testing Scenarios

Here, we present two Scenarios, one for measuring the effect of Voltage on average air velocity and the other for measuring the effect of gap distance for average air velocity.

1. Effect of voltage on air velocity:

   In this scenario, the gap distance between electrodes is fixed and equals 28mm, The applied voltage on electrodes is varied from 18KV to 23KV and the average air velocity is calculated in the region $d \times (0.27) mm^2$, the wire electrode radius is 0.075mm, the aluminum foil thickness is 0.01mm with rounded edges of radius 0.05mm and the side length is 150mm.

2. Effect of gap distance on air velocity:

   In this scenario, the Applied voltage on the electrodes is fixed at 20KV, the gap distance is varied between 26mm to 38mm and the average air velocity is calculated in the region $d \times (0.27) mm^2$, the wire electrode radius is 0.075mm, the aluminum foil thickness is 0.01mm with rounded edges of radius 0.05mm and the side length is 150mm.

7.5 Measures of effectiveness

The aim of this paper is to provide and test the accuracy of the model, so the only measure of effectiveness is the relative error between the simulation and the real data

$$Error = \frac{\sum |u_{calculated} - u_{experimental}|}{\sum |u_{experimental}|} \tag{7.1}$$

Where:

* $u_{calculated}$ is the velocity results from simulation.

* $u_{experimental}$ is the real experimental velocity.

8 Conclusion

As a Conclusion, we got to a model through which we could define the corona discharge phenomenon which is a wire-to-cylinder model known as the lifter, and to get results for this model we focused our work on two axes:

1. **Hardware axis:**
    - We designed two handmade lifters using home-based materials
    - We made our high-voltage power supply to ionize the air to exploit the thrust of the corona.
    - But after too many attempts, we failed to make the lifter fly although there was a wind that could be felt it was weaker than to be tested.
    - We think this may relate to some specs we didn't consider in our lifter of the power supply.
2. **Software axis:** To simulate the corona phenomenon, we employed three different software tools:
    (a) Comsol whose results weren't so accurate.
    (b) CST but unfortunately, we didn't get the correct results using it.
    (c) Matlab On the other hand, we utilized the finite difference method in Matlab to solve the equations, and we obtained a satisfactory simpler model and found:
        i. A very small error in the relationship of voltage and velocity which was around 0.7114%
        ii. A larger error in the relation of velocity and gap distance of about 6.012%
        iii. This model works accurately in smaller gap distances and begins to diverge for larger gap distances.
        iv. The relation of Voltage and velocity is an incremental linear relationship, which is a simple relationship.

9 Future work

Moving forward, our future work aims to gain a deeper understanding of the complex physics underlying the corona discharge phenomenon. We plan to develop more precise models that account for the effects of zero gravity. Additionally, we intend to make progress in the following areas:

1. **Hardware** With more time, we could figure out how to improve the wind and catch the bug in our tests, improve the power circuit to get a higher voltage that will give us better results that can be measured, in the long term we hope to enhance the control and maneuverability of the lifter to transform it into a fully-controlled drone.

2. **Software** We recognize the need to improve our utilization of the software tools we used in our simulations, specifically:

   (a) Comsol

   (b) CST

   We intend to simulate additional models and compare the results to identify any flaws in our current model and achieve the most accurate representation of the corona discharge phenomenon possible in order to achieve the dream of a plane without wings.

10 Bibliography

[1] Rytis Nykštelis. *Study of Ion propulsion technology and possible practical applications*. PhD thesis, Kauno technologijos universitetas, 2021.

[2] GHEORGHE Camelia, SEBEA Mihai, et al. The economic and social benefits of air transport. *Ovidius University Annals, Economic Sciences Series*, 10(1):60–66, 2010.

[3] Vincent Rawlin, James Sovey, John Hamley, Thomas Bond, Michael Matranga, and John Stocky. An ion propulsion system for nasa's deep space missions. In *Space Technology Conference and Exposition*, page 4612, 1999.

[4] Moshe Einat and Roy Kalderon. High efficiency lifter based on the biefeld-brown effect. *AIP Advances*, 4(7), 2014.

[5] Manés F Cabanas, Francisco P González, Andrés S González, Moisés R García, and Manuel G Melero. Analysis of the efficiency of the electrohydrodynamic propulsion based on the biefeld-brown effect for manned and unmanned aircrafts. *Applied Sciences*, 12(6):2997, 2022.

[6] Gary V Stephenson. The biefeld brown effect and the global electric circuit. In *AIP Conference Proceedings*, volume 746, pages 1249–1255. American Institute of Physics, 2005.

[7] Hisaichi Shibata, Yasumasa Watanabe, Ryosuke Yano, and Kojiro Suzuki. Numerical study on fundamental characteristics of electro-hydrodynamic thruster for mobility in planetary atmosphere. *TRANSACTIONS OF THE JAPAN SOCIETY FOR AERONAUTICAL AND SPACE SCIENCES, AEROSPACE TECHNOLOGY JAPAN*, 12(ists29):Pe_5–Pe_9, 2014.

[8] Thomas B Bahder and Chris Fazi. Force on an asymmetric capacitor. *arXiv preprint physics/0211001*, 2002.

[9] Ping Huang, Zhuo-yue Xie, Peng Liu, Da-peng Leng, Jin-pao Zheng, and Sen Wang. Ionic wind simulation of wire-aluminum foil electrode structure lifter in 2-d space. *IEEE Transactions on Plasma Science*, 50(3):566–573, 2022.

[10] Ma Chen, Lu Rong-De, and Ye Bang-Jiao. Surface aerodynamic model of the lifter. *Journal of Electrostatics*, 71(2):134–139, 2013.

[11] Arthur Brown. *Towards Practical Fixed-Wing Aircraft with Electroaerodynamic Propulsion*. PhD thesis, Massachusetts Institute of Technology, 2023.

[12] Nicolas Gomez-Vega, Haofeng Xu, James M Abel, and Steven RH Barrett. Performance of decoupled electroaerodynamic thrusters. *Applied Physics Letters*, 118(7), 2021.

[13] Haofeng Xu, Yiou He, and Steven RH Barrett. A dielectric barrier discharge ion source increases thrust and efficiency of electroaerodynamic propulsion. *Applied Physics Letters*, 114(25), 2019.

[14] Ping Huang, Zhuo-yue Xie, Peng Liu, Da-peng Leng, Jin-pao Zheng, and Sen Wang. Ionic wind simulation of wire-aluminum foil electrode structure lifter in 2-d space. *IEEE Transactions on Plasma Science*, 50(3):566–573, 2022.

[15] Daniel S Drew, Nathan O Lambert, Craig B Schindler, and Kristofer SJ Pister. Toward controlled flight of the ionocraft: a flying microrobot using electrohydrodynamic thrust with onboard sensing and no moving parts. *IEEE Robotics and Automation Letters*, 3(4):2807 2813, 2018.

[16] Filippo Cichocki, M Merino, E Ahedo, M Smirnova, A Mingo, and M Dobkevicius. Electric propulsion subsystem optimization for "ion beam shepherd" missions. *Journal of Propulsion and Power*, 33(2):370 378, 2017.

A Appedix: Matlab Code

```
clear;
clc;
%% Geometry
rc = 0.125 ; %wire elctrord radius im (mm)
tf = 0.01; %aluminum foil thickness in (mm)
d = 28; %gap distance
L = 0.15; % side length of the triangle in (m)
%% Constants
epsilon0 = 8.854e-12;
E0 = 3.31e6;
delta = 1;
epsilon =1; %roughness
mobility = 0.000215;
%mobility of air ranging from 2.15 to 1.45 cm^2/V.s


%% Mesh and gird
nx = 150;
ny = 1000;
xmin = -2;
xmax = 2;
ymin = 0;
ymax = 60;

x1 = linspace(xmin,-0.04,nx/3);
x2 = linspace(-0.0384, 0.04, nx/3);
x3 = linspace(0.0416, xmax, nx/3+1);
x = [x1 x2 x3];
%x = linspace(xmin,xmax,150);

y1 = linspace(ymin,50-d-0.04,  ny/5);
y2 = linspace(50-d-0.0404,50-d+0.04, ny/5);
y3 = linspace(50-d+0.0404,49.95, ny/5);
y4 = linspace(49.9505,50.05, ny/5);
y5 = linspace(50.0505, ymax, ny/5);
y = [y1 y2 y3 y4 y5];
%y =linspace(ymin,ymax,1000);
[X ,Y] = meshgrid(x,y);
nx = length(x);
```


```
ny = length(y);
%% Inializations
BoundaryMask1 = zeros(ny,nx);
BoundaryMask2 = zeros(ny,nx);
rhoq = zeros(length(y),length(x));
V = zeros(length(y), length(x));
rhoq(:,:) = 2.3256e-13;
%Assuming constant charge distrbution rhoq = sigma/mobility
for ii = 1:nx-1
        for jj = 1:ny-1
                x= X(jj,ii);
                y= Y(jj,ii);
                if (x)^2 + (y-50)^2 < rc^2
                        BoundaryMask1(jj,ii) = 1;
                end
                if  abs(x) < tf && y < sqrt(tf^2-x^2) +(50-d)
                        BoundaryMask2(jj,ii) = 1;
                end
        end
end
%% Values of VC 18KV to 23KV
% Loop through different values of Vc
%Vc_values = linspace(18000, 23000, 1000);
% Vary Vc from 18 kV to 23 kV
%Vi_values = [17548 , 18548, 19548, 20548 21548 22548];
% Vary Vc from 18 kV to 23 kV
Vi_values = 19794;
results = cell(length(Vi_values), 5); % Store results for each Vc value
rc = rc*1e-3; % rc is now in (m)
for k =1:length(Vi_values)
       Vi = Vi_values(k);
       V(:,:) = Vi/2; %
       for ii = 1:nx
           for jj = 1:ny
                if BoundaryMask1(jj,ii) == 1
            V(jj,ii)= Vi;
                end
                if  BoundaryMask2(jj,ii) == 1
                        V(jj,ii) = 0;
                end
```


```
80            end
81        end
82        rhoq(:,:) = 2.3256e-13;
83            %Assuming constant charge distrbution rhoq = sigma/mobility
84
85      for iter = 1:1000
86         Vold = V;
87                %rhoq_old=rhoq;
88         for ii = 2:nx-1
89             for jj = 2:ny-1
90                 if BoundaryMask1(jj,ii) == 1
91                   V(jj,ii)= Vi;
92
93                 elseif  BoundaryMask2(jj,ii) == 1
94                              V(jj,ii) = 0;
95                 else
96                     dx = 0.5*(1e-3)* (X(jj,ii+1)- X(jj,ii-1));
97                     dy = 0.5*(1e-3)* (Y(jj+1,ii)- Y(jj-1,ii));
98                     if dx == 0 || dy == 0
99                         disp('Dividing By zero');
100                    end
101                        V(jj,ii) = 0.5 * (1/(1/dx^2+1/dy^2))*(...
102                        (V(jj+1,ii)-V(jj-1,ii))/dy^2 + ...
103                        (V(jj,ii+1)-V(jj,ii-1))/dx^2);
104
105                end
106            end
107        end
108        if (max(abs(V(:) - Vold(:))) < 1e-6)
109            disp('Iam Here');
110            break;
111        end
112     end
113     Ex = zeros(size(V));
114     Ey = zeros(size(V));
115     ux = zeros(size(V));
116     uy = zeros(size(V));
117     for ii = 1:nx-1
118             for jj = 1:ny-1
119                 dx = (1e-3)* (X(jj,ii+1)- X(jj,ii));
```


```
                dy = (1e-3)* (Y(jj+1,ii)- Y(jj,ii));
                 if dx == 0 || dy == 0
                        disp('Dividing By zero when calculating grad');
                        disp(ii);
                        disp(' ');
                        disp(jj);
                 end
                Ey(jj,ii) = -(V(jj+1,ii) - V(jj,ii))/dy;
                Ex(jj,ii) = -(V(jj,ii+1) - V(jj,ii))/dx;
                ux(jj,ii) = Ex(jj,ii)*dx*dy;
                uy(jj,ii) = Ey(jj,ii)*dx*dy;
            end
    end
    results{k, 1} = V; % Potential difference
    results{k, 2} = Ex; % Electric field in x-direction
    results{k, 3} = Ey; % Electric field in y-direction
    results{k, 4} = mobility*ux; %Velocity in x direction
    results{k, 5} = mobility*uy; %Velocity in y-direction
end
%% Final results
Velocity_array= zeros(size(Vi_values));
Vc_values = Vi_values + 452; % Original VC values

for k = 1:length(Vi_values)
    ux = sum(results{k,4}(:));
    uy = sum(results{k,5}(:));
    % Divde by small region of intrest (gap distance*0.26)
    u = sqrt(ux^2 + uy^2)/((d*0.27)*(1e-6))*3*L;
        %3 is the sides of the triangle
    disp(u);
    Velocity_array(k)= u;
end
%figure;
%plot(Vc_values,Velocity_array);
%title("Velocity Vs Voltage");
%xlabel("Voltage");
%ylabel("Average Velocity");
```


B Appendix: Template of latex code

```
\documentclass[a4paper,11pt,table]{article}
\usepackage{notoccite}
\usepackage[numbers,sort&compress]{natbib}
\usepackage[utf8]{inputenc}
\usepackage{graphicx}
\usepackage{amsthm,amsfonts,amsmath}
\usepackage{esint}
\usepackage[table]{xcolor}
\usepackage{tikz}
\usetikzlibrary{positioning}
\usetikzlibrary{calc}
\usepackage[export]{adjustbox}
\usepackage{subcaption}
\usepackage{arabtex}
\usepackage{array, multirow}
\usepackage{tabularx, tabulary, tabu, longtable}
\usepackage[margin=1in,includefoot]{geometry}
\usepackage{fancyhdr}
\usepackage{utf8}
\setcode{utf8}
\usepackage{pgfplots}
\pgfplotsset{compat=1.18, width=10cm}

\usepackage{mathptmx}
\usepackage{esint}
\usepackage{enumitem}
\usepackage{setspace}
\usepackage{lipsum}
\usepackage{fancyvrb}
\usepackage{wrapfig}
\usepackage[colorlinks=false,hidelinks]{hyperref}
\usepackage{listings}
\usepackage[toc]{appendix}
\usepackage[nottoc,numbib]{tocbibind}
\usepackage{listings}


```


```
\usepackage{calc}
\usepackage{eso-pic}


\newcommand{\myframe}{
\begin{tikzpicture}[overlay,remember picture]
    \draw [line width=1pt,rounded corners=15pt,double]
        ($ (current page.north west) + (1cm,-1cm) $)
        rectangle
        ($ (current page.south east) + (-1cm,1cm) $);
\end{tikzpicture}
}
%\renewcommand{\tocloftpagestyle}{fancy}
\pagestyle{fancy}
\fancyhead{}
\setlength{\headheight}{14pt}
\fancyhead{\myframe}
\fancyfoot{}
\fancyfoot[c]{\vspace{6pt}\thepage\
}
\renewcommand{\headrulewidth}{0pt}
\renewcommand{\footrulewidth}{0pt}
\fancyfoot[R]{
        \vspace{0.1pt}
          \includegraphics*[scale=0.2]{images/team_icon.png}
}
\setlength{\footskip}{40pt}
\fancyfoot[L]{
        \vspace{6pt}
        \textcolor{gray}{\textit{ We Scare Because We Care}
}}
\definecolor{mymauve}{rgb}{0.58,0,0.82}
\lstset{
        %language = matlab,
        backgroundcolor=\color{white},   % choose the background color
            basicstyle=\footnotesize\ttfamily,      % size of fonts used for
                the code
        %mathescape,
        numbers = left,
        numberstyle = \small,
```


```
        numbersep = 5pt,
  breaklines=true,                 % automatic line breaking only at whitespace
  %captionpos=b,                    % sets the caption-position to bottom
  commentstyle=\color{green},    % comment style
% escapeinside={\%*}{*)},          % if you want to add LaTeX within your code
  keywordstyle=\color{blue},       % keyword style
  stringstyle=\color{mymauve},     % string literal style
  showstringspaces=false,
}


%-------------------------------------------------------------------------
\numberwithin{equation}{section}

\begin{document}
\newcommand{\mytitlename}{Research Paper}%Here Put the titlename(Task Name)
\input{pages/Title_page}

\pagenumbering{roman}
\input{tasks/Abstract}
\newpage

{\pagestyle{plain}
\tableofcontents
\listoffigures
\listoftables
\cleardoublepage
}

\setstretch{1.5}
\newpage
\hspace{\parindent}
%%%%%%%% Here Add your code or file %%%%%%%%%%%%%%%%%
\pagenumbering{arabic}
\setcounter{page}{1}
\input{tasks/problem_defintion}
\input{tasks/literature_review}
\newpage
\input{tasks/modelling/modeling_and_methodology}
\pagebreak
```


```
\input{tasks/results and simulation/intro}
\input{tasks/results and simulation/ResultsHardware}
\input{tasks/results and simulation/results_simulation}
\pagebreak
\input{results_testing_scenarios}
\newpage
\input{tasks/Future_work}
%%%%%%%%%%%%%%%%%%%%%%%%%%%%%%%%%%%%%%%%%%%%
\pagebreak
\newpage
\bibliographystyle{unsrtnat}
\bibliography{references/references}%add your refrences to this file
%\myframe
\newpage
\appendix
\input{Code}

\pagebreak
\section{Appendix: Template of latex code}
\lstinputlisting[language={[latex]TeX}]{main.tex}
\end{document}
```